Scientific paper

Preparation, Characterization and Catalytic Activity of NiO_x and NiO_x/ZrO_2 for Oxidation of Phenol in Aqueous Solution

Dimitar Petrov,[1,*] Stoyanka Christoskova,[1] Maria Stoyanova,[1] Vanina Ivanova[1] and Daniela Karashanova[2]

[1] *Department of Physical Chemistry, University of Plovdiv 24, Tsar Asen Str., 4000 Plovdiv, Bulgaria*

[2] *Institute of Optical Materials and Technologies, Bulgarian Academy of Sciences 109, Acad. Georgy Bonchev Str., 1113 Sofia, Bulgaria*

** Corresponding author: E-mail:petrov_d_n@abv.bg tel: +35 932 261206, fax: +35 932 261403*

Received: 25-03-2014

Abstract

In the present study bulk NiO_x and supported NiO_x/ZrO_2 catalysts have been prepared. The bulk NiO_x was synthesized using the precipitation-oxidation method with reverse order of precipitation while deposition-precipitation technique was used for the preparation of zirconia supported catalyst. The as-prepared samples were characterized by means of XRD, HRTEM, SAED, IR-spectroscopy, and chemical analyses. It was found that under the applied synthesis procedure nanosized and highly dispersed oxide materials with high active oxygen content were obtained. The catalytic activity and selectivity of these oxide catalysts have been studied in reaction of low-temperature oxidation of phenol in aqueous phase. The effects of several parameters such as catalyst amount, temperature and solution pH on the degradation efficiency of the process were also investigated. Experimental results demonstrated that phenol could be completely degraded under all reaction conditions, except at pH = 12.

Keywords: Phenol; Complete oxidation; Oxide catalysts; SAED; FTIR; Reaction kinetics

1. Introduction

Wastewater treatment is one of the most important area of environmental protection due to the fact that various organic pollutants are consistently produced and discharged into the environment and thus could induce considerable damages for the ecosystems. Therefore, development of efficient and cost-effective methods and technologies for complete destruction of such water contaminants has received a great attention in the last decades. Phenol and its derivatives, commonly present in many industrial effluents (e.g. from chemical, petrochemical, and pharmaceutical industries) represent an important class of environmental water pollutants due to their toxicity, comparatively more refractory to natural degradation and ability of formation of higher-molecular aromatic compounds.[1] Therefore, phenol is usually used as a model pollutant for wastewater treatment studies.[2–6]

Conventional technologies such as biological, thermal and chemical treatments have been applied for removing organic compounds from wastewaters. The biodegradation is represented as an environmentally friendly and non expensive method of treatment. However, its application is limited for effluents that contain high organic load and/or non-biodegradable compounds such as phenol and its derivatives.[7] Thermal incineration is applicable for almost complete destruction of concentrated and toxic organic waste streams, but it requires very high energy and presents considerable emissions of other hazardous by-products such as dioxins and furans.[8,9] Chemical methods such as adsorption, precipitation and flocculation are not widely used because of the need of a post-treatment stage.[10]

Advanced oxidation processes (AOPs) are alternative pollutants destructive technologies that have the potential to completely destroy harmful non-biodegradable or-

ganic contaminants in water. Typical examples of AOPs include Fenton and photo-Fenton oxidation process,[11,12] catalytic wet air oxidation (CWAO),[13,14] ozonation,[15,16] photo-catalytic oxidation[17] that are successfully used for the removal of phenol. Among the various AOPs processes, heterogeneous catalytic oxidation has some advantages such as operation at mild conditions with high energy efficiency.[18]

ZrO_2 is increasingly used as a catalytic support due to its several useful properties.[19] In a recently reported article it has been found that ruthenium catalyst prepared by impregnation on CeO_2-ZrO_2 support, show high activity and selectivity in the phenol oxidation.[20] At temperature of 413 K and under air pressure of 4 MPa phenol mineralization around 100 % was obtained within 100 h of reaction. Moreover, it has been mentioned that Ru/ZrO_2-CeO_2 catalyst possesses the possibility for practical use.[21] Zirconia supported Pt and Pd catalysts were found very promising for the low-temperature destructive oxidation of phenol with molecular oxygen in aqueous medium.[22] However, the increasing price of the noble metals limits their application as catalysts for industrial use.

The present paper aims to synthesize and characterize novel bulk and zirconia supported NiO_x catalytic systems in accordance with the scientific fundamentals of preparing ecological catalysts for fast and complete oxidation of phenol with air at ambient conditions.

2. Experimental

2. 1. Preparation of Catalysts

In developing the scientific fundamentals of the method for synthesis of new Ni-oxide catalytic systems (bulk and supported) we were guided by the main requirements for low-temperature environmental catalysts for complete oxidation of organic compounds under ambient conditions. The catalytically active phase should be characterized by high dispersity, high content of over-stoichiometric active oxygen, high oxidation degree and octahedric coordination of metallic ions, low energy of the surface cation- oxygen (M – O) bond and presence of OH – groups in their composition. The preparation of oxide catalysts, according to the requirements pointed above, depends strongly both on the initial compositions and the experimental conditions of their synthesis.

The synthesis of the bulk NiO_x samples was carried out by the precipitation-oxidation method with reverse order of precipitation in combination with ultrasound stimulation realized by ultrasound homogenizer UP100H. The stimulation of the synthesis by ultrasound cavitation provides, from the one hand, conditions for more efficient homogenization of the reaction mixture, and from the other, is a prerequisite for the preparation of highly dispersive and nano-sized systems with higher specific surface. The latter contributes to increasing the number of accessible catalytic centres for substrate adsorption and catalyst activation, which in its turn favors the reaction kinetics. The details of the synthesis are described in the paper of Christoskova et al.[23]

The supported oxide system NiO_x/ZrO_2 was prepared by deposition-precipitation technique. Solid ZrO_2 (Merck) was suspended in a fixed volume of 0.1 M aqueous solution of $Ni(NO_3)_2.6H_2O$, in an amount necessary to achieve an atomic ratio of Ni:Zr = 1:1, followed by dropwise addition of a mixture of 4 M NaOH and NaOCl at constant stirring by the ultrasonic homogenizer to yield a black precipitate. The latter was allowed to age in the mother solution for 24 hours, followed by filtration, washing with distilled water to a negative reaction towards Cl^- ions and neutral pH. The precipitate was dried at 105 °C to constant mass (the sample was marked as NiO_x/ZrO_2 –fresh). Part of the prepared catalyst was calcined in air at 300 and 600 °C, respectively for 4 hours in a program-controlled electric furnace LM312.11C at a heating rate of 2 °C/min. The thermally treated samples were labelled as NiO_x/ZrO_2 – 300 and NiO_x/ZrO_2 – 600, respectively.

In order to determine the phase composition of the samples, the content of active oxygen, the strength of the M – O bond and the coordination of the metal cation, the synthesized catalytic systems were characterized by means of X-ray diffraction (XRD), Fourier transform infrared spectroscopy (FTIR), and chemical analyses. The morphology of the as prepared samples was studied by transmission electron microscopy (TEM).

The bulk NiO_x catalyst was characterized in our previous investigations using a set of physicochemical techniques for investigation of solids such as XRD, XPS and EPR.[23] Therefore, some of the corresponding spectra are not illustrated in the present work.

2. 2. Characterization of Catalysts

XRD was performed using a X-ray diffractometer TUR-MA 62, operating at U = 37 kV, Cu Kα radiation (λ = 1.5406 Å) and I = 20 mA. The diffractometer was supplied with a computer-controlled goniometer (HZG - 3), scanning step of the spectrum of 0.04 ° and collection time of impulses – 1.2 s. The samples were scanned in 2θ range within 10–80 °. The phase identification was carried out using JCPDS database.[24] The experimental XRD spectra were processed with »PowderCell« program for determining the content of the registered phases, as well as of the lattice parameters of each of the monitored phases.

The FTIR spectra were taken on a Vertex 70 spectrophotometer (Bruker), with 2 cm^{-1} resolution, in KBr pellets (1 mg of the corresponding sample in 100 mg KBr).

Structural analysis of the samples was performed using high resolution JEOL JEM 2100 electron microscope operating at an accelerating voltage of 200 kV. Two ba-

sic regimes of microscope mode were used – bright field transmission microscopy (BF TEM) and selected area electron diffraction (SAED).

The chemical analysis of the synthesized catalysts included determination of the total active oxygen content (O*), expressed in % and g-at g^{-1} and of their specific surface area.

Active oxygen is the amount of over-stoichiometric oxygen in the oxide above that corresponding to the lowest stable oxidation state. The content of total active oxygen was determined iodometrically.[25] For this purpose a proper amount of the sample (0.1 g ± 0.0001) was dissolved in diluted (1:10) sulphuric acid containing 2 g solid KI at constant stirring. The liberated iodine was titrated with 0.1 N solution of $Na_2S_2O_3$ in the presence of starch as indicator. The relative standard deviation of the method amounts to 4.71 %.

The content of O*, in g-at g^{-1}, was calculated according to the following formula:

$$O^* = \frac{N\,V\,mgE_{O_2}}{m16} \quad (1)$$

or in % according to :

$$O^* = \frac{N\,V\,mgE_{O_2}}{m}.100 \quad (2)$$

where: N – normality of the titrant; V – volume of the consumed titrant solution, cm^3; m – catalyst mass, g; mgE_{O_2} = 0.008 miligram equivalent O_2.

The surface area of the studied catalytic systems was determined using an adsorption method. This method is based on the determination of the iodine amount (I_2, g) which is necessary to cover the measured surface with a monomolecular layer. The method is express and precise and its accuracy is of the same order as that of the classical BET method.

The amount of iodine adsorbed on the catalyst surface was determined titrimetrically. The procedure was as follows: a proper amount of the catalyst (0.50 ± 0.01 g) was placed in a flask and 25 cm^3 0.05 M iodine solution in chloroform was added. The flask was shaken for 2 hours. The catalyst was filtered and an aliquot of the filtrate (10 cm^3) was titrated against 0.1 N sodium thiosulfate using starch as indicator (V_1, cm^3). A 10 cm^3 0.05 M iodine solution was parallelly titrated (V_2, cm^3).

The amount of adsorbed iodine (G) was calculated according to formula (3), and the specific surface area (S) according to formula (4):

$$G = \frac{(V_2 - V_1)N\,mEq_{I_2}\,25}{10}, g \quad (3)$$

$$S = \frac{G\,N_A\,\omega}{M_{I_2}\,m}, m^2 g^{-1} \quad (4)$$

where: mEq_{I_2} = 0.127; N_A–Avogadro constant; ω –surface area occupied by one iodine molecule (taken 9 × 10^{-20} m^2); M_{I_2} – molecular weight of the iodine, and m – mass of the catalyst.

Point of zero charge (pH_{PZC}) of the samples was determined using the mass titration method.[26]

2. 4. Catalytic Oxidation Procedure

The process of low temperature (25–35 °C) liquid phase oxidation of phenol by air at atmospheric pressure was carried out in a thermostated 150 cm^3-cell volume under constant stirring by a magnetic stirrer. At these conditions in the reaction volume an uniform environment is ensured for all parameters defining the system state: operating temperature, phenol concentrartion, pH (pH = 6.0 or pH = 12.0), amount of dissolved oxygen. Kinetic studies were investigated with model solutions with initial 50 mg dm^{-3} concentration of phenol. The choice of concentration is consistent with the actual content of phenol in industrial wastewaters. The amount of catalyst in the different experiments varied within the range 2–5 g dm^{-3}. In all experiments the following procedure was used: 100 cm^3 of phenol solution was saturated by air at atmospheric pressure for 20 minutes followed by the addition of an appropriate amount of catalyst. The catalysts were used in powder form to maximise the number of accessible active sites on the surface of catalysts and thus to enhance the oxidation rate. The process was conducted at continuous bubbling of air into the system, resulting in steady concentration of the dissolved oxygen.

In order to clarify the effect of temperature on the activity and selectivity of the tested catalytic systems the oxidation was conducted at two temperatures 25 °C and 35 °C.

The change in phenol concentration and that of the intermediate products of its oxidation was followed by UV – Vis spectral analysis and high-performance liquid chromatography (HPLC). The UV–Vis spectra as well as their second derivatives (D2) were recorded by two-beam scanning UV-Vis spectrophotometer (Cintra 101) in the range of 200–600 nm. The use of derivative spectroscopy (D-Sp) ensures more precise analysis of multi-components systems. The spectral measurements were carried out in a 5-mm quartz cuvette and bidistilled water was used as a reference. The phenol concentration was determined on the basis of the measured absorption intensity at λ_{max} = 268 nm using a calibration graph.

The HPLC analyses were performed using a computerized system for liquid chromatography Knauer, Germany, which consists of two isocratic pumps with a mixer and equipped with PDA and fluorescence (RF-10 Axl) detectors. The components separation in the analyzed samples was carried out on an analytical column Purospher (Merck) RP C_{18} (250 × 4.6 mm i.d., 5 μm). The analysis was conducted in gradient conditions. Solutions contai-

ning water, acetonitrile and acetic acid were prepared. The mobile phase A was a mixture of 90 parts of 1 % aqueous solution of acetic acid and 10 parts of the mobile phase B. The latter was prepared by mixing 99 parts of acetonitrile and 1 part of 1 % aqueous solution of acetic acid. The flow rate was 1 ml/min. For better separation of phenols a gradient at room temperature: 100% A from 0–20 minutes to 30% A, from 20–30 minutes to 0 % A, from 30 to 31 minutes to 100% A was used. The volume of the analysed sample was 20 μl.

Chemical Oxygen Demand (COD) content of the initial phenol solution and those at given time of its oxidation was determined by the reflux colorimetric method using a Spectroquant® CSP/COD cell test (Merck) and a NOVA 400 UV-Vis spectrometer (Merck, Germany). The COD values of the initial phenol solution and those at given time of its degradation were determined by reflux colorimetric method using a Spectroquant® CSP/COD cell test (Merck AG). Sample solution (2 mL) was pipetted into the COD tube and digested at 148 °C for 2 hour in an Spectroquant® TR 420 COD reactor. COD concentration was measured colorimetrically at λ = 420 nm using a NOVA 400 UV-Vis spectrometer (Merck AG).

The amount of dissolved oxygen and pH of the solution were controlled by a multi-functional apparatus Ino Lab Multi 740.

The efficiency of the heterogenous catalytic oxidation of phenol was assessed both by the degree of PhOH conversion (α, %) and the extent of COD removal (%), calculated by the following equations:

$$\alpha = \frac{Co - C}{Co} 100 \quad (5)$$

$$COD\,removal = \frac{[COD]o - [COD]}{[COD]o} 100 \quad (6)$$

where: $C°$ and C are the initial phenol concentration and concentration of phenol at a given time of the oxidation reaction, respectively (mol dm^{-3}); [COD]o and [COD] are the initial and current COD concentrations, respectively (mg dm^{-3}).

The kinetics of phenol degradation was evaluated by the first order kinetic model:

$$k = \frac{1}{t} \ln \frac{C_o}{C} \quad (7)$$

3. Results and Discussion

3. 1. Powder X-ray Diffraction

The data obtained from the X-ray analysis of ZrO_2, NiO_x/ZrO_2 – fresh, NiO_x/ZrO_2 – 300 and NiO_x/ZrO_2 – 600 are presented in Figure 1. It was found that the bulk NiO_x is amorphous and therefore its diffractogram is not shown. The amorphous character of the bulk sample determines the chemical and structural isotropy of the active sites on catalyst surface which is a prerequisite to high selectivity in oxidation processes. Phase composition, average crystallite size (D) calculated using the Debbye-Scherrer equation, and lattice parameters of the unit cell of the synthesized samples were determined from the experimental XRD profiles. Data obtained are summarized in Table 1.

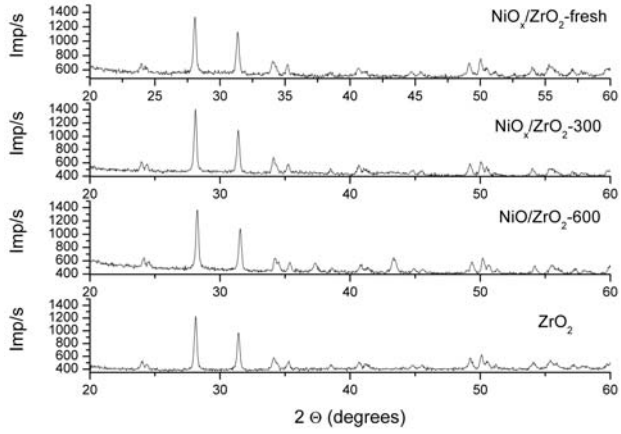

Fig. 1. Diffraction patterns of ZrO_2 and NiO_x/ZrO_2 – fresh and calcinated samples

The X-ray diffraction pattern of the ZrO_2 support confirms its monoclinic structure (JCPDS 88-2390). In the XRD spectrum of NiO_x/ZrO_2 – fresh only diffraction lines of ZrO_2 are registered. Moreover, the intensities of the ZrO_2 patterns are not reduced after deposition of the active component, indicating that crystallites size of the NiOx is retained.

Although the relatively high content of Ni in the supported sample, the absence of distinct reflections for Ni-containing oxide or oxy-hydroxy (NiOOH) phases could be due to the amorphous character of the deposited active phase, as well as to the formation of highly-dispersed oxide layer on the support surface.

Our previous studies on the thermal stability of bulk NiO_x by derivatographic and X-ray analyses demonstrated that NiO phase was formed during the thermal treatment of the sample at 300 °C.[23] In contrast, the X-ray diffraction pattern of NiO_x/ZrO_2 – 300 again shows the presence only of single-phase oxide material – ZrO_2. However, in the diffractogram of the supported sample, calcined at 600 °C, besides the characteristic lines of the support, two new peaks at 2θ = 37.24° and 43.24° were registered. These peaks are indexed to reflections of the (1 1 1) and (2 0 0) planes of face-centered cubic crystal structure of NiO (JCPDS 47-1049), confirming the formation of NiO phase. The higher temperature of NiO phase formation in the NiO_x/ZrO_2–600 sample could be attributed to the benefi-

Table 1 Phase composition and crystallographic properties of catalysts

Sample	Phase composition	D, nm	Lattice parameters of the unit cell, Å
ZrO_2	ZrO_2	34	a = 5.144; b = 5.208; c = 5.307'
NiO_x/ZrO_2 – fresh	ZrO_2	45	a = 5.141; b = 5.204; c = 5.308'
NiO_x/ZrO_2 – 300	ZrO_2	48	a = 5.138; b = 5.197; c = 5.303'
NiO_x/ZrO_2 – 600	ZrO_2 (91 %)	42	a = 5.142; b = 5.204; c = 5.310'
	NiO (9 %)	25	a = 4.173

cial role of ZrO_2 support to improve the thermal stability of the catalyst. This in turn suggests that a part of the active oxygen is still maintained even at higher temperatures (near 300 °C), thereby extending the practical application of the studied catalytic systems in oxidation reactions in gas phase.

3. 2. TEM and SAED Analyses

TEM and the corresponding SAED micrographs of the catalytic active phase NiO_x are presented in Fig. 2. The nanoparticles have spherical-like form and diameter in the range 5 nm – 20 nm forming large agglomerates that contain hundreds of particles. It has been found that they correspond to monoclinic $Ni_{15}O_{16}$ phase [PDF 72-1464].

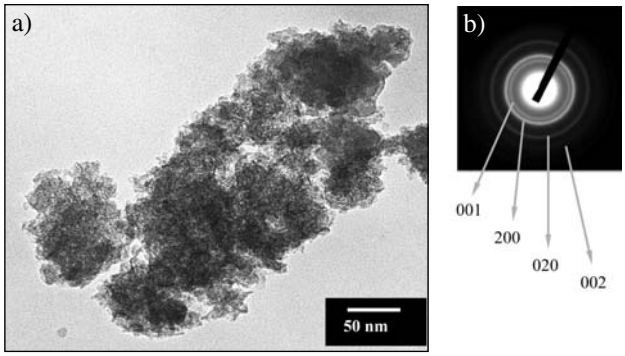

Fig. 2. TEM (a) micrograph and SAED (b) patterns of NiO_x

Although not detectable by the XRD technique, the presence of NiO_x nanoparticles in NiO_x/ZrO_2 – fresh can be confirmed using HRTEM and SAED regimes of the transmission electron microscope. In Fig. 3a is presented the TEM image of the catalytic system NiO_x/ZrO_2 – fresh. Two types of morphologically-different particles are observed in the investigated sample. The first type of particles are electronically-dense, apparently well faceted, with dimensions in the range 50 nm – 300 nm, indicated with No 1 in the image. Other (No 2 in the image), being with diameter of about 5 nm–10 nm, form large aggregates numbering hundreds of particles clustered around the large ones.

In order to determine the phase composition of the sample diffractions were made seperately for both particle types. For this purpose, the diffraction signal was captured by the two selected areas marked with circles in Fig. 3a: 1 – for the large particles and 2 – for the smaller ones. The diffractograms of both particle types are presented in Fig. 3b and 3c. It is seen that the large-walled particles are indeed monocrystalline, as we supposed by the morphology of the particles. The analysis of the diffraction pattern shows that they consist of ZrO_2 [PDF 37–1484], in this case directed to the zone axis [121] and correspond to the material used as a carrier of the supported catalyst. The small particles also have crystalline structure, but because of their small size and aggregate formation, in the surface of the aperture, a signal from a great number of them has been included and the cumulatative diffraction signal is found to be similar to that of polycrystalline sample (Fig. 3c). After the indexation of the diffraction pattern it has been found that it correspods to the $Ni_{15}O_{16}$ phase.

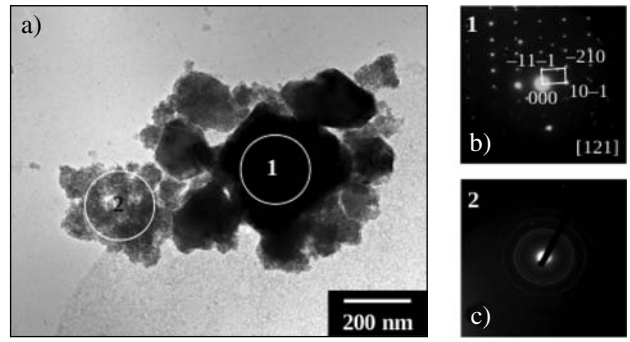

Fig. 3. (a) TEM micrograph of the catalytic system NiO_x/ZrO_2 and (b, c) the corresponding SAED for the two areas, marked with 1 and 2.

Fig. 4 shows the HRTEM micrograph of part of an aggregate presented in Fig. 3. The edge of the large ZrO_2 particle and a number of $Ni_{15}O_{16}$ particles arranged to it are observed. It is clearly seen that the small particles have also well-defined facets, visible at high magnifications of the microscope (600k and more). High-resolution fringes corresponding to the two types of structures are visualized and the values of their inter-planar distances are indicated in the figure.

The results of the SAED examinations revealed the presence of a non-stoichiometric nickel oxide ($Ni_{15}O_{16}$), confirming the results from the preliminary investigations with derivatographic as well as chemical analysis. The non-stochiometry in this case provides the presence (avai-

lability) of active oxygen which is required for the activity of the catalyst. It has been confirmed that the bulk NiO_x exists in the form of nanoparticles with size in the range from 5 nm to 20 nm, which provides large specific surface area. Their arrangement around the ZrO_2 carrier as loose agglomerates ensures access to their surface. Through microscope observation revealed that these complex agglomerates, consisting of large ZrO_2 nanoparticles and multiple NiO_x nanoparticles around them, are well dispersed in the sample, which also performs another important condition for the operation of the catalyst.

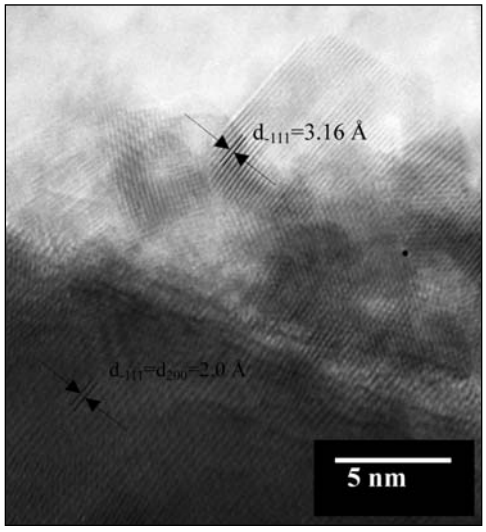

Fig. 4. HRTEM micrograph of an agglomerate shown in fig. 3.

3. 3. Chemical Analyses

Our previous study showed that bulk NiO_x is characterized by a high content of active oxygen (7–8 %), 80 % of it being localized on the catalyst surface.[23] This oxygen is highly reactive and is responsible for the heterogeneous liquid phase oxidation of the substrate even at room temperature. The presence of over-stoichiometric (*i.e.* active) oxygen in the sample is a result of the applied method of synthesis, whose key moment is the simultaneous process of precursor formation $Ni(OH)_2$ and its subsequent oxidation by NaOCl. As a result of the electron transfer between the hydroxide and the oxygen from the oxidant, the oxidation state of the metal ions is increased and a high concentration of electrophilic oxygen species (O^-, O_2^{2-}, O^{2-}), i.e. of over-stoichiometric (active) oxygen on the oxide surface is provided. These effects are of great importance to the complete oxidation catalysts.[27]

The active oxygen is formed as a result of the chemisorption of nascent oxygen, generated from the NaOCl decomposition in strongly alkaline medium catalyzed by Ni^{2+}– ions, on the surface area of the oxide system.

The chemical analyses showed that the ZrO_2, NiO_x/ZrO_2 – 300, and NiO_x/ZrO_2 – 600 do not contain active oxygen, which was confirmed also by the IR spectra of the samples. The reduced content of O* in NiO_x/ZrO_2 – fresh (2.6 %) compared to the bulk catalyst is attributed to the considerably lower content (30 wt %) of the catalytically-active phase NiO_x in the fresh supported catalyst. Moreover, the amount of this active oxygen was further reduced upon thermal treatment of NiO_x/ZrO_2 – fresh at 300 °C and higher temperatures. It should be noted that incorporation of O* in the studied samples expands their application as catalysts for complete oxidation of organic compounds under mild conditions (room temperature and atmospheric pressure). This fact makes possible their direct use for solving ecological problems associated with wastewater treatment for organic contaminants removal.

3. 4. FTIR Spectroscopy

In Figures 5–7 are shown the IR spectra of the bulk NiO_x, NiO_x/ZrO_2 – fresh and ZrO_2, respectively.

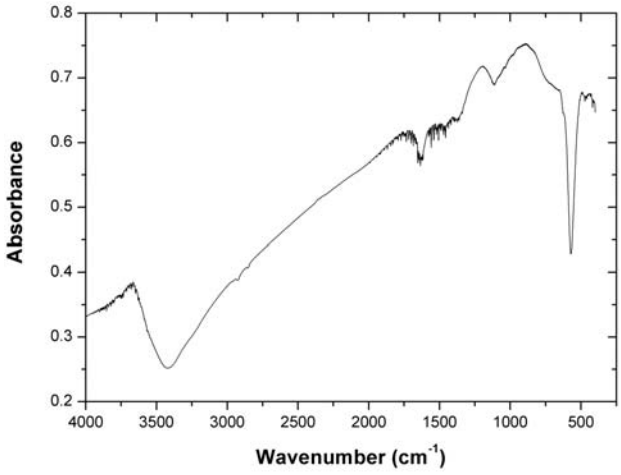

Fig. 5. IR spectrum of bulk NiO_x

A characteristic feature of the IR spectrum of NiO_x is the presence of a broad intensive band at 572 cm^{-1}. This band (registered at frequencies, higher than those assigned to the M – O bond vibrations in the corresponding hydroxides – 460 cm^{-1}) is due to the stretching vibration of the surface M – O bond and accounts for the presence of active oxygen in the samples, thereupon its intensity is proportional to the content of O*. Such band is not present in the IR spectrum of the ZrO_2 support, confirming the absence of active oxygen in the sample (fig. 7).

The intensity of the band at 572 cm^{-1} in the IR spectrum of the supported NiO_x/ZrO_2 – fresh catalyst is lower suggesting lower content of active oxygen (fig. 6). These data are consistent with the results of the chemical analysis of the samples.

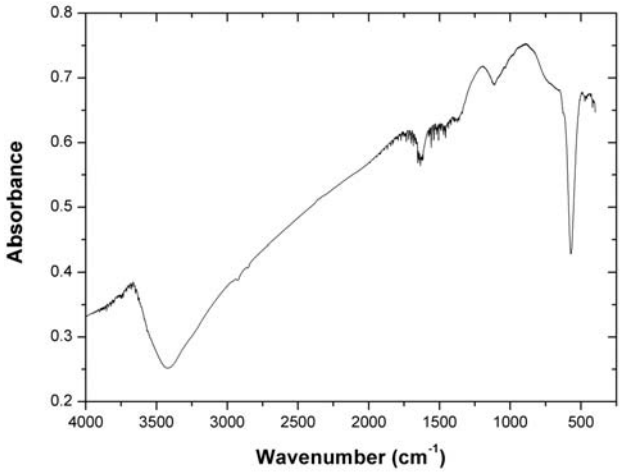

Fig. 6. IR spectrum of NiO_x/ZrO_2 – fresh.

It is known that the strength of the bond between surface cation and oxygen is the main factor providing catalytic activity of oxide catalysts in oxidation reactions. The oxygen atoms can be bound in two ways in the structure of the transition metal oxides: through covalent bonds with two adjacent metal atoms (M-O-M) or double σ–π bonds only with single atom (M = O). The type of oxygen bonding in oxides is distinguished in the IR spectra. The stretching mode of M = O bond which is stronger than the M-O bond is registered in the range between 900 and 1100 cm^{-1}, while that of M-O bond appears between 600 and 900 cm^{-1}.[28] In the presented spectra a band in a former spectral region was not observed. It is experimentally found that oxide catalysts containing the M = O bond in their structure oxidize selectively organic substances whereas those with M – O bond exhibit high catalytic activity in the reactions of complete oxidation.[29] Based on the results from the IR spectral characterization of the studied catalytists it could be suggested a high activity of the synthesized samples in reactions of complete oxidation.

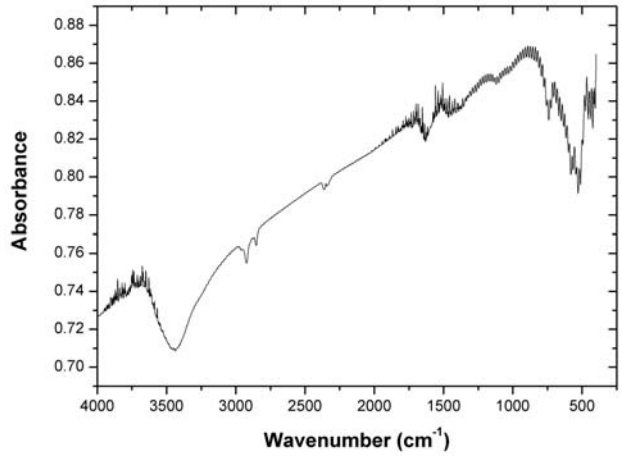

Fig. 7. IR spectrum of pure ZrO_2

The infrared spectra of ZrO_2, NiO_x, NiO_x/ZrO_2 – fresh catalysts also show an absorption band with a maximum centered about 3370 cm^{-1} (O-H stretching), together with a band at 1627 cm^{-1} (H-O-H bending). The band at 3370 cm^{-1} can be ascribed to hydroxyl groups bonded through hydrogen bonds, whereas the band at 1627 cm^{-1} corresponds to adsorbed molecular water. It is also known that the formation of hydrophilic precipitates depends on the precipitation procedure. The incorporation of OH – groups in the composition of the oxide systems (as a result of the applied inverse order of precipitation) is appropriate, since they are invloved in the oxidation mechanism of the studied reaction. Moreover, the reverse order of precipitation does not provide conditions for the proceeding of secondary topochemical reactions between the formed precipitate and the solution leading to the formation of basic salts.

3. 5. Specific Surface Area

The specific surface area of the NiO_x was found to be 28.7 $m^2 g^{-1}$, and that of NiO_x/ZrO_2 – fresh is 8.6 $m^2 g^{-1}$. The lower specific surface area of the latter compared to that of the active phase is due to the lower specific surface area of the bare ZrO_2, varying about 1–3 $m^2 g^{-1}$,[30–32] as well as to the low percentage loading of catalytically active NiO_x phase (weight percentage ratio of NiO_x:ZrO_2 = 30:70).

3. 6. Low Temperature Oxidation of Phenol in Aqueous Solutions Over Bulk NiO_x and Supported NiO_x/ZrO_2 Catalysts

In preliminary control test was found that chemical oxidation of phenol by air takes place very slowly in the absence of catalyst, resulting in less than 3% phenol degradation within 60 min. A negligible reduction in the phenol concentration was also registered during heterogeneous oxidation in the presence of bare support and only around 10 % of degradation was achieved after 60 min of reaction. It should be noted that a similar PhOH removal efficiency was also attained in adsorption test, indicating that ZrO_2 is catalytically inactive with respect to substrate oxidative degradation. However, under the same conditions a significant enhancement of the rate of phenol oxidation was observed using NiO_x/ZrO_2 – fresh as catalyst.

Figs. 8 and 9 show typical UV-vis spectra and their second derivatives obtained during heterogeneous catalytic oxidation of phenol over NiO_x/ZrO_2 – fresh under the experimental conditions employed.

It is seen from the figures that the synthesized sample NiO_x/ZrO_2-fresh demonstrates high catalytic activity at ambient conditions, resulting in about 80% phenol removal efficiency at 10 min and almost complete conversion of phenol (more than 98 %) in 20 min at 5 g dm^{-3} catalyst loading. Furthermore, the second derivative spectrum of the

solution recorded after oxidation for 20 min indicates the absence of aromatic intermediates in the reaction mixture. However, the COD removal within this reaction period was about 71.2% which implies that under operating conditions phenol is not completely mineralized and the further oxidized intermediate products such as low molecular weight carboxylic acids still present in the solution.

It should be emphasized that in another control experiment conducted without bubling of air in the solution (depletive oxidation) the concentration of phenol decreased only around 21% in the first ten minutes and was kept constant afterwards, i.e. about four-fold lower removal rate compared to that of heterogeneous catalytic oxidation was observed. In the meantime, a new absorbance peak at about 244 nm appeared in the UV-vis specrum of the sample collected after 10 min (not shown), implying that an intermediate compound is being formed during the process. Therefore, it may be speculated that the observed decrease of phenol concentration in this case is due to the oxidative destruction of phenol rather than the nondestructive adsorption of PhOH on the surface of the catalyst. Actually, at pH 6.0 the surface sites of NiO_x/ZrO_2-fresh are positively charged since the pHpzc of catalyst was found to be 7.1. On the other hand, given that pKa value of phenol is 9.99, at pH used in our experiment phenol primarily exists in its unionized form. Based on these facts, it is considered that the electrostatic interaction between phenol and NiO_x/ZrO_2-fresh could be ignored under given conditions and most probably the non-electrostatic surface complexation may take part during the contact between catalyst and phenol. Thus, the phenol degradation in the absence of an oxidant could be assumed to occur due to the presence of active oxygen in the NiO_x/ZrO_2-fresh, which was confirmed by the about 10-fold lower O* content of the catalyst after the depletive oxidation as compared to that of the fresh sample. On contrary, when the reaction was conducted in the presence of oxygen the amount of active oxygen in the NiO_x/ZrO_2-fresh remains unchanged after the reaction completed. Since the oxidation of phenol without a catalyst was found to occur very slowly, it can be concluded that the active oxygen of the catalyst is directly involved in the oxidation process, while the oxygen from air re-oxidizes the partially reduced surface of the catalyst. The negligible catalytic activity demonstrated by samples calcined at 300 °C and 600 °C (less than 5% phenol conversion within 60 min) further confirmed the above assumption.

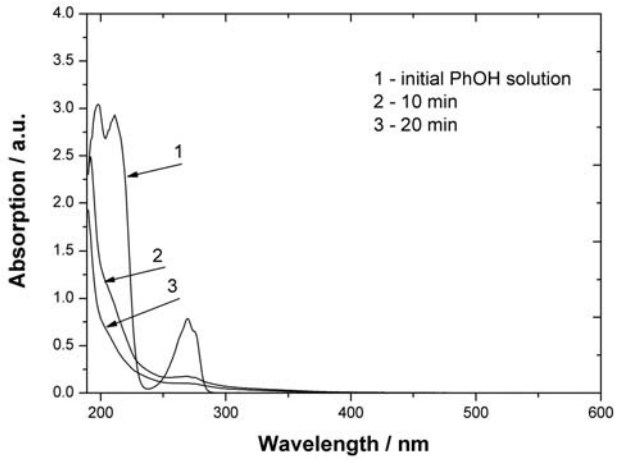

Fig. 8. UV-vis spectral changes of phenol during heterogeneous oxidation over NiO_x/ZrO_2 – fresh (C_{cat} = 5 g dm^{-3}; C_{PhOH} = 50 mg dm^{-3}; t = 25 °C; pH = 6.0)

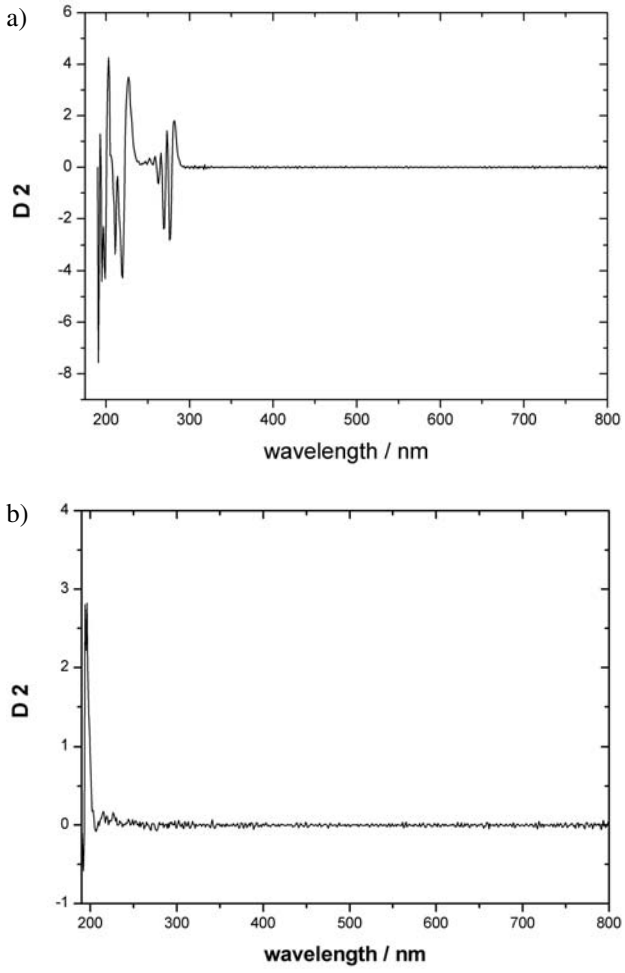

Fig. 9. Second derivative spectra of phenol solution before (A) and after oxidation for 20 minutes (B) over NiO_x/ZrO_2 – fresh

Further details on the high selectivity of the catalytic system with respect to phenol complete oxidation were also obtaind by HPLC analysis. Phenol and its oxidation products were identified using a fluorescence detector due to its higher sensitivity compared to the PDA detector. HPLC chromatograms of samples taken at definite times of the oxidation process are illustrated in Fig. 10.

The results of HPLC analysis confirmed the UV-spectroscopic observation of almost complete phenol conversion over NiO_x/ZrO_2 – fresh within 20 min. However, a small amount of an intermediate compound was detected in the reaction mixture, which further is also degraded and af-

ter 20 min present only in trace amounts. The intermediate was identified as hydroquinone by comparing the retention time of the corresponding peak in the chromatogram of the reaction mixture with that of the standard solution, containing phenol and major products of its partial oxidation. Hydroquinone was not detected in the UV- spectra (λ_{max} = 290 nm) probably due to its low concentration, which is below the detectable limit of this analytical method.

The reusability of NiO_x/ZrO_2 – fresh in three successive runs was investigated with the recycling of the catalyst under the same reaction conditions. After the degradation was finished, the used catalyst was collected by filtration, washed thoroughly with double distilled water and dried overnight before the next run. It was found that the phenol degradation rate in the first and second runs was the similar and only dropped slightly in the third run. However, in the latter run the phenol removal was still about 94% after 20 min thus demonstrating stable performance of the NiO_x/ZrO_2 – fresh catalyst in the studied reaction.

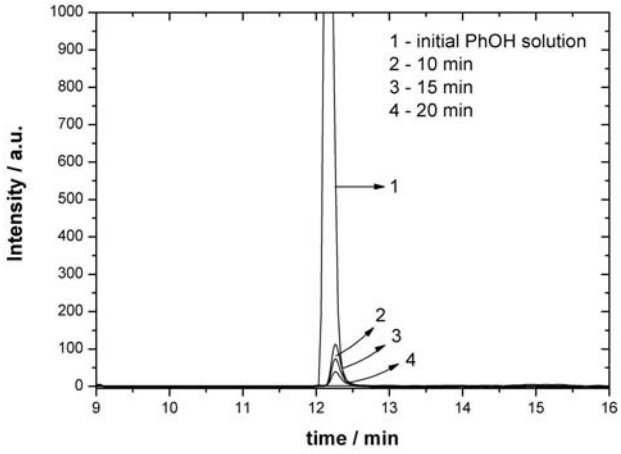

Fig. 10. High-perfomance liquid chromatograms of phenol solution during catalytic degradation over NiO_x/ZrO_2 – fresh. (C_{cat} = 5 g dm^{-3}; C_{PhOH} = 50 mg dm^{-3}; t = 25 °C; pH = 6.0)

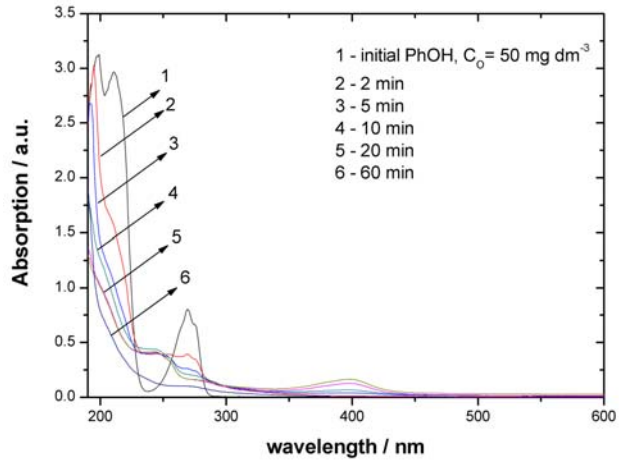

Fig. 11. UV – vis absorption spectra of phenol solution during catalytic oxidation on NiO_x.(m = 0.156 g; C_{PhOH} = 50 mg dm^{-3}; t = 25 °C; pH = 6.0)

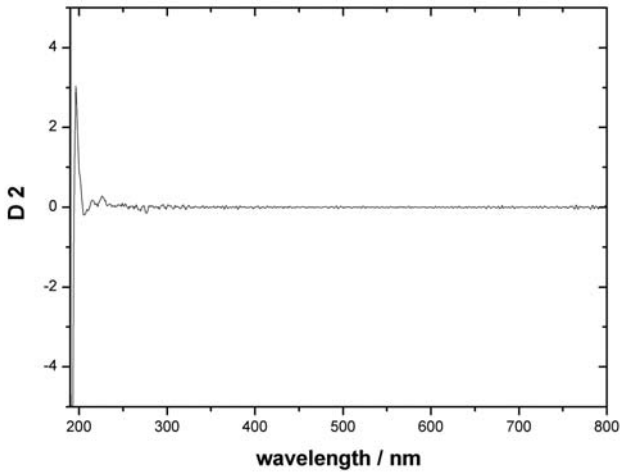

Fig. 12. Second derivative spectrum in 60 min of phenol oxidation with active phase NiO_x (m = 0.156 g; C_{PhOH} = 50 mg dm^{-3}; t = 25 °C; pH = 6.0)

In order to assess the impact of the carrier ZrO_2 on the catalytic behavior of the supported catalyst, oxidation of phenol over bulk NiO_x was performed under the same conditions except the amount of catalyst which was equivalent to the content of the active phase in NiO_x/ZrO_2 – fresh (30 wt.%).

The UV-vis spectra of the reaction mixture, collected at certain degradation times and their second derivatives are depicted in Figs. 11 and 12, respectively. It is evident that along with the slower reaction kinetics compared to the oxidation over NiO_x/ZrO_2 – fresh, the electronic absorption spectra show different profiles. During the oxidation process in the presence of non-supported NiO_x, in parallel with the gradual decrease in the intensity of the band at 268 nm, new absorption bands with maxima at 244, 275 and 400 nm appear, which is indicative of intermediates formation. The latter are subsequently oxidized slow and complete phenol oxidation is achieved for 60 minutes. The absence of a distinct isobestic point in the spectrum in Fig. 10 demonstrates the formation of more than one intermediate compounds. According to literature data,[33] the band at λ_{max} = 244 nm is attributed to *p*-benzoquinone, while that at λ_{max} = 275 nm may be due to the presence of catechol and/or hydroxyhydroquinone in the reaction mixture which makes difficult their identification only by UV spectral analysis. It is noteworthy that at the beginning of the oxidation process over NiO_x another intermediate compound is also formed (λ_{max} = 400 nm), that according to some authors could be attributed to the formation of dimers.[33] Meanwhile, as has been observed by using of NiO_x/ZrO_2-fresh, without bubling of air in the solution initially the phenol oxidation occurs as fast as the reaction carried out in the presence of oxygen and then a strong decrease of the oxidation rate with time was registered. Chemical analysis of NiO_x after the depletive oxidation experiment again showed a significant decrease in the active oxygen content (around 1 %) thus implying that as-prepared NiO_x being a solid oxidant itself.

Due to higher activity of $NiOx/ZrO_2$ – fresh compared to that of non-supported catalytically active phase, further investigations on the effects of main operating conditions such as pH, amount of catalyst, and temperature on the catalytic behavior and efficiency of the supported catalyst for the oxidative destruction of phenol were performed.

The UV- spectra of samples of the reaction mixture taken in the course of the oxidation process conducted at pH = 12.0 as well as the spectrum of the initial phenol solution without pH adjustment (6.0) are illustrated in Fig. 13.

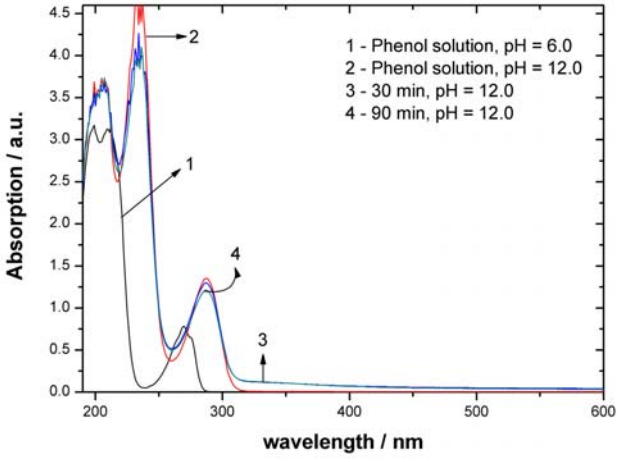

Fig. 13. UV-spectrum of oxidation of phenol over NiO_x/ZrO_2 – fresh at pH = 6.0 and pH = 12.0 and after 30 and 90 min of the oxidation process at pH = 12.0 (C_{cat} = 5 g dm^{-3}, t = 35 °C)

The presented spectra evidence that the phenol oxidation do not take place in alkaline medium. Furthermore, the comparison of the UV-spectra of phenol solution at pH 6.0 and pH 12.0 reveals a batochromic shift of the absorption maximum of phenol in alkalime medium, which is due to the formation of phenolate anion (λ_{max} = 286 nm). Hence, the adsorption of phenol onto the NiO_x/ZrO_2 – fresh at pH 12 is also considered to be restricted due to the repulsion between the negatively charged phenol species and negatively charged surface of the catalyst.

Similar effect of pH has been observed during the liquid phase catalytic oxidation of phenol using the active phase NiOx [21], assuming a similar mechanism of the catalytic oxidation process on the bulk and supported on ZrO_2 catalysts. According to this mechanism, the oxidation reaction is initiated by dissociative adsorption of phenol on the surface of catalyst through tearing of an H atom off from the phenolyc hydroxyl group. The cleaved H atom formed with the active oxygen of the catalyst highly-reactive surface OH radicals, which readily attack the phenol molecule and causes its destruction. The active oxygen is continually renewed by re-oxidation of the reduced catalyst by oxygen from air, which was continuously bubbled in the reaction mixture. These results give us reason to suggest that the catalytic oxidation reaction follows the Mars-van Krevelen reduction- oxidation mechanism. Since at pH = 12.0 phenol is in the form of phenolate anion in the solution, this makes impossible the generation of OH radicals and, respectively, the oxidation of the substrate.

The effect of catalyst amount and temperature on the kinetics of the catalytic process is evaluated by the rate constant of the reaction and the degree of phenol degradation. Fig. 14 presented the kinetic curves obtained during catalytic oxidation of phenol at 25 °C using three different concentrations of $NiOx/ZrO_2$ – fresh along with phenol degradation profiles obtained in the course of chemical oxidation with air and the heterogeneous catalytic oxidation over bare support.

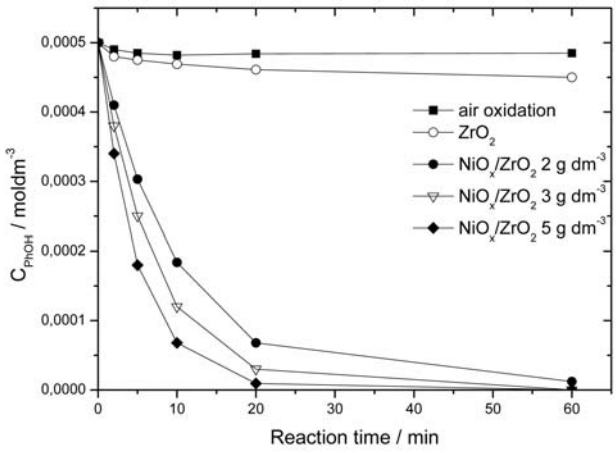

Fig. 14. Kinetic curves of the PhOH oxidation at t = 25 °C with NiO_x/ZrO2-fresh

The enhanced rate of phenol degradation resulted by increasing of catalyst concentration from 2 to 5 g dm^{-3} could be ascribed to the increased amount of the generated OH radicals because of higher amount of the available active oxygen in the larger catalyst mass. The linear plots of $\ln(C_o/C)$ versus time (fig. 15) indicate that the oxidative destruction of phenol over $NiOx/ZrO_2$ – fresh followed the first-order kinetics with respect to phenol concentration.

Continual re-oxidation of the reduced catalyst by oxygen from continuously bubbling air is considered to provide steady-state concentration of active oxygen on the catalyst surface as well as to maintain a constant concentration of dissolved oxygen in the liquid phase (8.6 mg/l) throughout the oxidation process. This fact gives us grounds to assume that the reaction rate becomes independent of the oxidant concentration under studied experimental conditions. Therefore, it could be suggested that the order of the reaction with respect to oxygen is zero.

The rate constants of the oxidation process determined at varying the NiO_x/ZrO_2 – fresh concentration and the temperature are listed in Table 2. The established linear dependence of the rate constant on the catalyst loa-

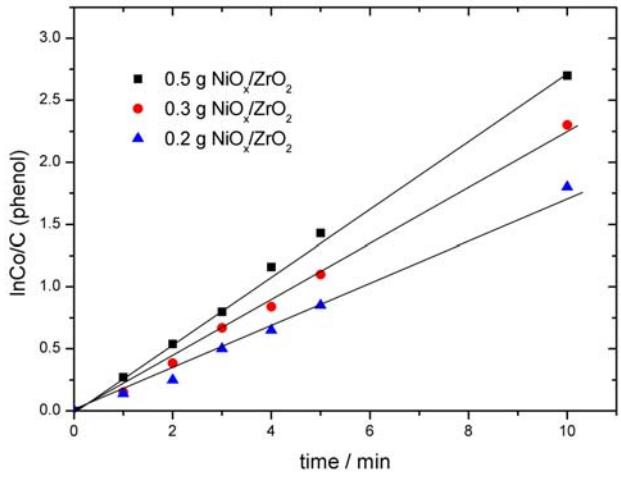

Fig. 15. Linear dependence $\ln C_o/C = f(t)$

ding at both temperatures indicates that the reaction is not controlled by external diffusion and moreover, it further supported the assumption that active oxygen of the catalyst takes part in the oxidation process.

Data regarding the influence of the reaction temperature and catalyst concentration on the efficiency of heterogeneous oxidation of phenol over NiO_x/ZrO_2 – fresh, expressed by the degree of phenol conversion are illustrated in Fig. 16.

The results show that at 35 °C and catalyst concentration of 5 g dm^{-3} complete conversion of phenol is achieved for 5 minutes.

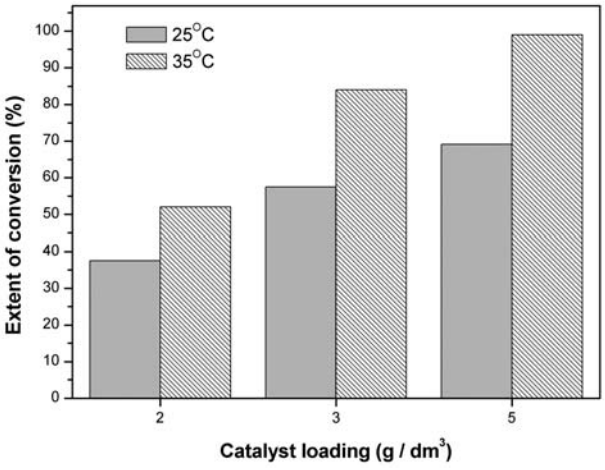

Fig. 16. Dependence of the degree of phenol conversion α on temperature and catalyst concentration after 5 min of oxidation

The degree of phenol mineralization in the course of its catalytic oxidation over NiO_x/ZrO_2 – fresh was also assessed by the parameter COD. It was found that under the experimental conditions (C_{cat} = 5 g dm^{-3}; C_{PhOH} = 50 mg dm^{-3}; t = 25 °C; pH = 6.0) used, 80.4 % COD removal was achieved for 20 minutes, which can be attributed both to trace amounts of non-oxidized hydroquinone in this reaction period and to traces of low-molecular carboxylic acids.

4. Conclusions

As a result of the proposed non-conventional synthesis, assisted by ultrasonic stimulation we obtained nano-sized, highly dispersed nickel-oxide catalytic systems, characterized by a high content of active oxygen, highest degree of oxidation of metal ions in octahedral coordination, that are main characteristics of low-temperature catalyst for complete oxidation. The use of ZrO_2 support increases the thermal stability of the obtained catalyst which is expected to expand its practical application as a catalyst not only for oxidation in liquid but also in gas phase reactions. The results of the catalytic experiments also show that ZrO_2 has substantial influence on the activity and selectivity of the supported catalyst in the reaction of low temperature oxidation of phenol by air in liquid phase. It was found that at all investigated reaction conditions, except at pH = 12, practically complete conversion of phenol is achieved in the presence both of the bulk and the supported catalysts. However, the catalytic performance of active phase NiO_x was considerably improved after deposition on ZrO_2, manifesting in faster phenol degradation rate and a higher COD removal efficiency. The results also show that increasing the amount of NiO_x/ZrO_2 – fresh and the reaction temperature affects strongly the efficiency of the oxidation process. Thus, at 35 °C and catalyst concentration of 5 g dm^{-3}, complete degradation of phenol is observed for 5 minutes, while 80.4 % COD removal within 20 min was attained. The supported catalyst also exhibited stable performance during the recycling tests.

5. Acknowledgements

Financial support from NSFB (Projects DFNI E01/7) and from University of Plovdiv Research Fund (Project NI HF-2013) is gratefully acknowledged.

Table 2 Effect of temperature and catalyst concentration on the reaction rate constant of phenol oxidation

Temperature, °C	First-order rate constants, k (min^{-1})		
	C_{cat} = 2 g dm^{-3}	C_{cat} = 3 g dm^{-3}	C_{cat} = 5 g dm^{-3}
25	0.10 ± 0.01	0.14 ± 0.01	0.20 ± 0.01
35	0.15 ± 0.02	0.20 ± 0.01	0.28 ± 0.02

6. References

1. A. Santos, P. Yustos, A. Quintanilla, S. Rodríguez, F. García-Ochoa, *Appl. Catal. B Environ.* **2002**, *39*, 97–113.
2. G. Ovejero, J. L. Sotelo, F. Martinez, L. Gordo, *Water Sci. Technol.* **2001**, *44*, 153–160.
3. P. Shukla, S. Wang, K. Singh, H. M. Ang, M. O. Tadé, *Appl. Catal. B Environ.* **2010**, *99*, 163 169.
4. S. Muhammad, E. Saputra, H. Sun, H. M. Ang, M. O. Tadé, S. Wang, *Ing. Eng. Chem. Res.* **2011**, *51*, 15351–15359.
5. F. Adam, J. T. Wong, E. P. Ng, *Chem. Eng. J.* **2013**, *214*, 63–67.
6. J. B. De Heredia, J. Torregrosa, J. R. Dominguez, J. A. Peres, *Chemosphere* **2001**, *45*, 85–80.
7. A. V. Vinod, G. V. Reddy, *J. Hazard. Mater. B* **2006**, *136*, 727–734.
8. M. Pera-Titus, V. García-Molina, M. A. Baños, J. Giménez, S. Esplugas, *Appl. Catal. B Environ.* **2004**, *47*, 219–256.
9. K. H. Kim, S. K. Ihm, *J. Hazard. Mater.* **2011**, *186*, 16–34.
10. A. Marco, S. Esplugas, G. Saum, *Water Sci. Technol.* **1997**, *35*, 321–327.
11. J. A. Zimbron, K. F. Reardon, *Water Res.* **2009**, *43*, 1831–1840.
12. M. Perez, F. Torrades, J. G. Hortal, X. Domenech, J. Peral, *Appl. Catal. B: Environ.* **2002**, *36*, 63–74.
13. F. Stüber, I. Polaert, H. Delmas, J. Font, A. Fortuny, A. Febregat, *J. Chem. Technol. Biotechnol.* **2001**, *76*, 743–751.
14. A. Quintanilla, A. F. Fraile, J. A. Casas, J. J. Rodríguez, *J. Hazard. Mater.* **2007**, *146*, 582–588.
15. S. H. Lin, C. H. Wang, *Environ. Technol.* **2003**, *24*, 1031–1039.
16. G. J. Makarand, L. S. Robert, *Water. Res.* **1982**, *16*, 33–938.
17. A. Babuponnusami, K. Muthukumar, *Chem. Eng. J.* **2012**, *183*, 1–9.
18. S. Muhammad, P. R. Shukla, M. O. Tadé, S. Wang, *J. Hazard. Mater.* **2012**, *215–216*, 183–190.
19. H. Wei, X. Yan, S. He, C. Sun, *Catal. Today* **2013**, *201*, 49–56.
20. J. Wang, W. Zhu, S. Yang, W. Wang, Y. Zhou, *Appl. Catal. B: Environ.* **2008**, *78*, 30–37.
21. L. F. Liotta, M. Gruttadauria, G. Di Carlo, G. Perrini, V. Librando, *J. Hazar. Mater.* **2009**, *162*, 588–606.
22. M. Sadiq, M. Ilyas, *Modern Res. Catal.* **2012**, *1*, 23–27.
23. St. G. Christoskova, N. Danova, M. Georgieva, O. Argirov, D. Mehandzhiev, *Appl. Catal A: General* **1995**, *128*, 219–229.
24. ICPDS - 19073–3273.
25. K. Nakagava, R. Konaka, T. Nakata, *J. Org. Chem.* **1962**, *27*, 1597–1601.
26. A. S. Franka, L. S. Oliveira, M. E. Ferreira, *Desalination* **2009**, *249*, 267–272.
27. A. Bielanski, J. Haber, Oxygen in Catalysis, Marcel Dekker Inc., New York, USA, **1991**.
28. A. Davidov, in: IR Spectroscopy in The Chemistry of Oxide's Surface, Khimia, Novosibirsk, USSR, **1984**.
29. F. Trifiro, I. Pasquon, *J. Catal.* **1968**, *12*, 412–416.
30. T. Tanuma, H. Okamoto, K. Ohnishi, S. Morikawa, T. Suzuki, *Appl. Catal. A : General.* **2009**, *359*, 158–164.
31. L. E. Davies, N. A. Bonini, S. Locatelli, E. E. Gonzo, *Latin Amer. Appl. Res.* **2005**, *35*, 23–28.
32. Is. Fatimah, K. Wijaya, K. H. Setyawan, *Bull. Chem. Reac. Eng. Catal.* **2008**, *3*, 9–13.
33. T. Ölmez-Hanci, I. Arslan-Alaton, *Chem. Eng. J.* **2013**, *224*, 10–16.

Povzetek

Z uporabo obarjalno-oksidacijske metode z obratnim zaporedjem obarjanja smo pripravili »bulk« NiO_x. Za pripravo ustreznega katalizatorja NiO_x/ZrO_2 pa smo uporabili usedalno-obarjalno tehniko. Pripravljene snovi smo kemijsko analizirali ter jih okarakterizirali s uporabo XRD, HRTEM, SAED in IR spektroskopije. Ugotovili smo, da z uporabo navedenih metod dobimo polidisperzne okside nano velikosti z visoko vsebnostjo aktivnega kisika. Njihovo katalitsko aktivnost in selektivnost smo proučevali z uporabo pri izvedbi reakcije popolne oksidacije fenola v vodni fazi pri nizki temperaturi. Izkazalo se je, da ta reakcija popolno poteče pri vseh izbranih pogojih razen pri pH = 12.